Some realities of field balancing

by Robert C. Eisenmann, P.E.
President
Machinery Diagnostics, Inc.
Minden, Nevada

While many turbomachinery rotors are successfully shop-balanced at low or high speed, some rotors can only be balanced in their casings in the field, using every technique, trick, and piece of information available to the specialist.

Most turbomachinery rotors are successfully balanced in slow speed shop balancing machines. This approach provides good access to all correction planes, and the option of performing multiple runs to achieve a satisfactory balance. It is generally understood that running at slow speeds with simple bearings or rollers does not duplicate the rotational dynamics of the field installation. Other rotors are shop balanced on high speed machines installed in vacuum chambers. These machines provide an improved simulation of the installed rotor behavior, due to the higher speeds and the use of bearings that resemble the normal running bearings. In these high speed chambers, the influence of blade and wheel aerodynamics is significantly reduced by operating within a vacuum.

Some machines, such as large steam turbines, often require a field trim balance, due to the influence of higher order modes or the limited sensitivity of the low speed balancing techniques.

There is also a small group of machines, which, except for component balancing, must be balanced in the field. These machines have segmented rotors, that are assembled concurrently with the diaphragms and/or casing. In these machines, the final rotor assembly is not achieved until most of the stationary elements are bolted into place. An example of this type of rotor is shown in Figure 1.

Machine configuration

This rotor consists of an overhung hot gas expander wheel, a pair of midspan compressor wheels, and three stages of overhung steam turbine wheels. A series of axial through bolts are used to connect the expander stub shaft through the compressor wheels and into the turbine stub shaft. This type of rotor assembly is similar to many gas turbine rotors. However, in this machine, the rotor must be built concurrently with the inner casing. Specifically, the horizontally split internal bundle is assembled with the titanium-aluminum compressor wheels, stub shafts, plus bearings and seals. End casings are attached, the expander wheel is bolted into position, and the three turbine stages are attached with another set of through bolts.

The eight rotor segments are joined with Curvic® couplings, which are identified as #1 through #7 on Figure 1. Even with properly ground and tight fitting

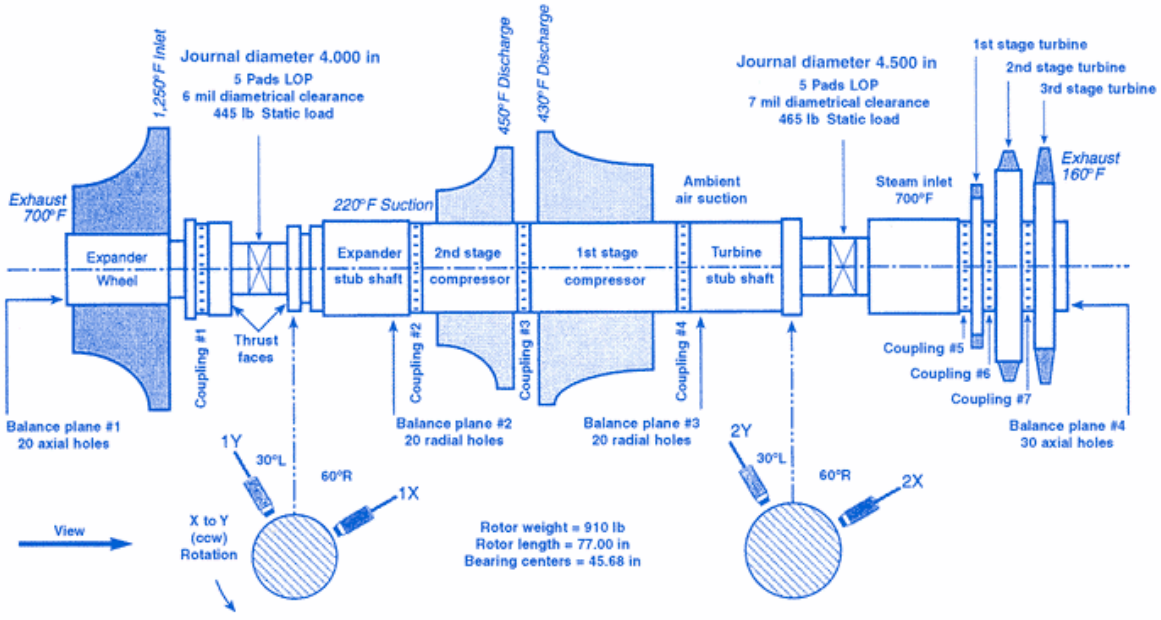

Figure 1
Expander-air compressor-steam turbine rotor and vibration transducer arrangement.

couplings, there is potential for relative movement of rotor elements. Although each of the rotor segments is component balanced, any minor shift between elements will produce a synchronous unbalance force. Since this unit operates at 18,500 rpm, a few grams of unbalance or a mil or two of eccentricity will result in excessive shaft vibration and a strong potential for machine damage.

Furthermore, the distribution of operating temperatures noted on Figure 1 reveals the complexity of the thermal effects that must be tolerated by this unit. The expander wheel inlet temperature is 677°C (1,250°F), and compressor discharge temperature is in excess of 221°C (430°F). The steam turbine operates with a 371°C (700°F) inlet temperature and a final exhaust temperature of 71°C (160°F).

By any definition, this must be considered a difficult rotor to deal with. More than one person has referred to this rotor as a "squirrel," meaning a rotor which responds erratically. On the positive side, this machine is a compact design that yields a high thermal efficiency. Therefore, when the unit is properly assembled, and balanced, it is very cost-effective to operate.

Field balancing this 413 kg (910 lb) rotor is achieved by adding or removing weights from a series of threaded holes in four balance planes (Figure 1). Balance Plane #1 contains 20 axial holes at the expander exhaust. Plane #2 and #3 each have 20 radial holes. They are located in two rows on the expander and turbine stub shafts, respectively. The outboard end of the turbine 3rd Stage wheel contains balance Plane #4 with 30 axial holes.

Shaft vibration measurements are made with Bently Nevada XY proximity probes (Figure 1). These radial probes are connected to a Bently Nevada 3300 Monitoring System, which in turn is connected to a Transient Data Manager® (TDM2) Communications Processor (CP). The CP sends static and dynamic signals from the monitors to a personal computer running TDM2 Software.

This instrumentation is used for monitoring, trending, and machinery diagnostics. The 3300 Monitors can automatically activate alarms when vibration setpoints are exceeded, and the computer system has additional Alert and Danger indications. This instrumentation also provides the steady state and transient vector data necessary for field trim balancing this complex rotor.

Balancing calculations

During shop balancing, it is easy to make a weight change; it is inexpensive to make a run, and there is little physical risk to the machinery or the operator. In the case of field balancing, it is often difficult to change weights, and it is generally expensive to make a full speed run. Furthermore, if an incorrect weight is used, the results may be hazardous to the machinery, and the health of the operator.

Each field balance shot should be a meaningful move, and should contribute to the overall database describing the behavior of the machine. Balancing behavior is based on the fundamental relationship between the shaft response and the applied force expressed by:

$$Response = \frac{Force}{Restraint} = \frac{Force}{Dynamic\ Stiffness} \qquad (1)$$

This general expression has many specific applications in rotor dynamics. Within the balancing discipline, the **response** is the measured shaft or casing **motion** and the **force** is the magnitude of the unbalance force. The **restraint** is the dynamic stiffness. Another way to view this term is to consider it as the sensitivity of the machine to rotor unbalance.

The variables in Eq.1 are vector quantities. That is, each parameter carries both a magnitude and a direction. If the vibration of a rotor is described by the A vector, with amplitude units of mil pp, and the unbalance magnitude is defined by the U vector with units of grams instead of force, then the sensitivity S vector carries the anticipated engineering units of gram/mil pp. Equation 1 may now be rewritten as follows:

$$A = \frac{U}{S} \qquad (2)$$

The vibration vector A is measured directly, and the problem resolves to one of determining the unbalance based upon an unknown Sensitivity vector. According to most sources, this problem was originally solved by E.L. Thearle in his 1934 ASME paper. He basically provided a way to practically determine the sensitivity vector. That procedure involves the addition of a known calibration weight to the rotor and determining the response vector C due to that calibration weight. If the calibration weight vector is defined by W, and the resultant vibration response vector of the rotor is defined as the $A+C$, Equation 2 may be expanded as follows:

$$A + C = \frac{U + W}{S} = \frac{U}{S} + \frac{W}{S} = A + \frac{W}{S}$$

or, by subtracting A from both sides,

$$C = \frac{W}{S}$$

This last expression may be solved for the sensitivity S vector:

$$S = \frac{W}{C} \qquad (3)$$

The S vector may now be combined with the initial vibration response vector in Eq. 2, and the unbalance vector computed. The concept has been around for over 60 years, and has been successfully applied on many machinery rotors.

The previous discussion covered only one measurement plane. The same logic may be applied to two or more measurement and correction planes. With respect to the current rotor under investigation, there are only two measurement planes, and four separate correction planes. This is different from most machines where the number of measurement and correction planes are equal.

Thus, the general form of eq 3 is:

$$S_{mp} = \frac{W_p}{C_{mp}} \qquad (4)$$

where m is the measurement plane and p is the weight correction plane.

The balancing technique of *"add a weight, make a run, take data, and do vector calculations"* generally produces acceptable results on many machines. However, this technique may fail on a complex rotor. A review of the balance history of the machine may help identify the correct technique.

Historical data review

A double overhung rotor with an appreciable midspan mass (such as Figure 1) has the potential for multiple resonances with both forward and reverse modes. In order to better understand the behavior of this machine, various historical data sets were reviewed. Fortunately, TDM2 data was available. This included steady state orbits, plus transient speed Bode and polar plots. From this data it was clear that reverse orbits appeared around 7,000 and 17,000 rpm. In addition, tabular lists of sampled vectors were also documented. **It was noted that the slow roll vectors were not repetitive, and this was a cause for concern.**

Previous field balancing activities on this machine were generally successful when a two step correction was used. The first step consisted of a balance at the process hold point of 14,500 rpm, using the outboard Planes #1 and #4. This was followed by a trim at 18,500 rpm on the inboard Planes #2 and #3 located next to the compressor wheels. It was evident that if the rotor wasn't adequately balanced at 14,500 rpm, it probably wouldn't run at 18,500 rpm.

For comparative purposes, the Sensitivity vectors from three different data runs were computed based upon steady state data at 14,500 rpm. These $\boldsymbol{S}$ vectors were computed in accordance with Eq. 4. The results are summarized in Table 1. The two shaded vectors in this table are of questionable accuracy, due to the fact that the differential vibration vector $\boldsymbol{C}$ was less than 0.1 mil pp. This small differential vibration is indicative of low sensitivity to the applied weight.

The $\boldsymbol{S}$ vectors in Table 1 have some similarities, but the variations are significant. For example, the magnitude of $\boldsymbol{S_{12}}$ varies from 22.6 to 76.4 gram/mil, and a 76° angular difference is noted. On $\boldsymbol{S_{24}}$, the amplitudes change from 24.2 to 14.9 gram/mil, but the angles reveal a 59° spread. **At this point, a preliminary conclusion might be reached that this rotor is nonlinear, and cannot be field balanced.** Clearly, additional information was needed to define the rotor behavior.

Process observations

Further examination revealed that vibration severity changed in accordance with the machinery operational state. Peak vibration amplitudes occur at a rotor critical (balance resonance) that appears between 7,600 and 8,100 rpm. This resonance displays the following characteristics versus operating conditions:

- Cold startup to 14,500 rpm
  Peak response of 2.0 to 5.0 mil pp
- Warm coastdown from 14,500 rpm
  Peak response of 4.0 to 5.0 mil pp
- Hot shutdown from 18,500 rpm
  Peak response of 6.0 to 8.0 mil pp

These amplitude variations, combined with changes in the rotor Synchronous Amplification Factor through the resonance, suggest a change in the damping term (Quadrature Dynamic Stiffness) of dynamic stiffness.

Furthermore, it was determined that the different operating conditions were directly associated with variations in shaft slow roll vectors, which were taken at 1,000 rpm. In all cases, the runout vectors for each cold startup, warm coastdown or hot emergency shutdown were consistent within each condition. When the rotor was shut down from a hot state, the slow roll vectors always returned to the same initial starting vectors as the rotor cooled. **Therefore, the apparent changes in slow roll were resolved.**

It was also determined that the previous vibration response vectors used for balancing were acquired at a process hold point of 14,500 rpm. Under this condition, the machine speed was held constant, but rotor and casing temperatures were changing as the process stabilized prior to continued startup of the plant. Next, the complete transient response picture needed to be added to this process data.

Transient data review

There is an adage that states, *"If your only tool is a hammer, then all of your problems begin to resemble nails."* This is very appropriate for this particular rotor. If the *"put a weight in and take a weight out"* balance technique is the only tool available, the results are often disappointing. This is evident from the spread in sensitivity vectors shown in Table 1. Attempting to balance a machine when these values keep changing is difficult at best. Many runs are required to attain a barely acceptable balance state.

It is quite clear that additional tools must be employed to properly field balance this machine. Certainly, the plant process observations discussed in the

S Vector	Data Set #1 (gram/mil @ deg)	Data Set #2 (gram/mil @ deg)	Data Set #3 (gram/mil @ deg)
S_{11}	20.3 @ 139°	16.2 @ 179°	*Not Available*
S_{12}	48.1 @ 34°	22.6 @ 309°	76.4 @ 233°
S_{13}	42.6 @ 211°	14.7 @ 177°	24.6 @ 200°
S_{14}	34.1 @ 259°	41.7 @ 289°	16.2 @ 305°
S_{21}	18.3 @ 308°	13.4 @ 345°	*Not Available*
S_{22}	19.1 @ 168°	18.5 @ 142°	18.6 @ 160°
S_{23}	32.3 @ 258°	20.2 @ 269°	31.2 @ 221°
S_{24}	24.2 @ 83°	20.3 @ 147°	14.9 @ 142°

Shaded vectors are of questionable accuracy due to small differential vibration vectors with calibration weights installed

Table 1
Sensitivity vectors based on steady state data at 14,500 rpm.

previous section are significant. However, this information must be supplemented by an examination of the variable speed (transient) vibration response data (Bode and polar plots), plus an understanding of the rotor critical (balance resonance) speeds, and mode shapes.

The vibration response from the installed proximity probes was extracted from the TDM2 database; a typical startup Bode plot is shown in Figure 2. This data displays the Y axis probes from both measurement planes. Both plots are corrected for slow roll runout. (Note: the Bode plots start at 4,000 rpm for better resolution.) Thus, the resultant data is representative of the true dynamic motion of the shaft at each of the two lateral measurement planes.

The major resonance occurs at approximately 7,800 rpm. Note that the process hold point at 14,500 rpm displays substantial amplitude and phase excursions. This is logically due to the heating of the rotor and casing, plus variations in "settle out" of the operating system (i.e., pressures, temperatures, flow rates, and molecular weights). **Although this process stabilization is a necessary part of the startup, the variations in vibration vectors negate the validity of this information for use as repetitive balance response data.**

At speeds above 14,500 rpm, there are additional vector changes, and a desirable *flat spot* (plateau) in the amplitude and phase curves does not appear. The only essentially flat area that provides consistent vibration vectors occurs in the vicinity of 14,000 rpm.

To test the validity of this conclusion, individual vectors at 14,000 rpm were extracted from the TDM2 transient startup files. These vibration vectors, in conjunction with the installed weights, were used to compute the sensitivity vectors in accordance with Eq. 4. The results of these computations are presented in Table 2. These vectors are directly comparable to the vectors discussed in Table 1. However, it is clear that the consistency of the ***S*** vectors among the three data sets is far superior in the results shown in Table 2. **Therefore, future balance corrections at this intermediate point were based upon the transient vectors acquired by the TDM2 System as the rotor passed through 14,000 rpm.**

The Bode plot in Figure 2 also exhibits a variety of amplitude and phase changes between 14,500 and 18,500 rpm. Other vector changes are visible as the machine approaches the normal operating speed of 18,500 rpm. Some of these changes are due to the influence of a backward mode around 17,000 rpm.

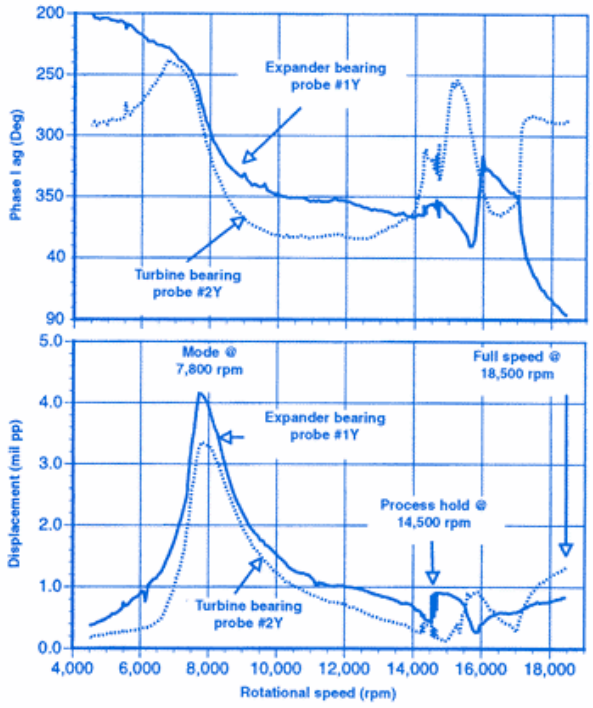

Figure 2
Runout-compensated Bode plot of Y-axis probes during typical machine train startup.

S Vector	Data Set #1 (gram/mil @ deg)	Data Set #2 (gram/mil @ deg)	Data Set #3 (gram/mil @ deg)
S_{11}	24.7 @ 144°	88.2 @ 188°	*Not Available*
S_{12}	125. @ 333°	38.2 @ 228°	42.4 @ 228°
S_{13}	31.8 @ 207°	20.8 @ 184°	22.9 @ 176°
S_{14}	21.8 @ 322°	36.1 @ 321°	30.7 @ 301°
S_{21}	24.9 @ 313°	21.6 @ 311°	*Not Available*
S_{22}	17.3 @ 167°	23.7 @ 175°	18.9 @ 178°
S_{23}	78.7 @ 299°	22.2 @ 221°	27.4 @ 232°
S_{24}	27.6 @ 147°	25.8 @ 166°	28.3 @ 164°

Shaded vectors are of questionable accuracy due to small differential vibration vectors with calibration weights installed

Table 2
Sensitivity vectors based on transient data at 14,000 rpm.

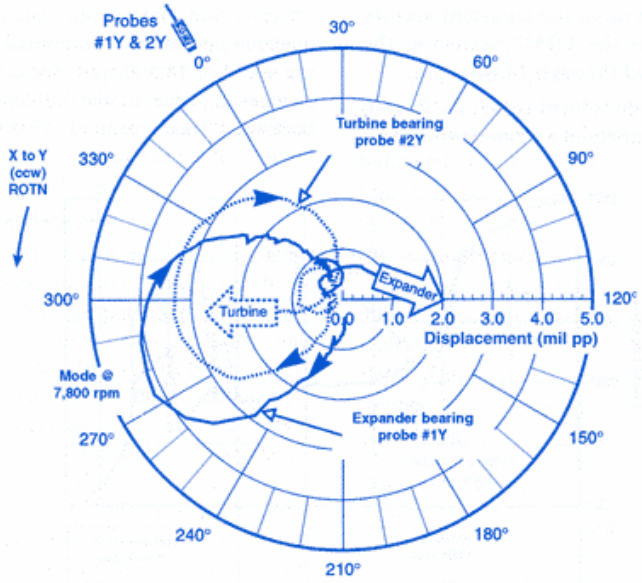

Figure 3
Runout-compensated polar plots of Y-axis probes during typical machine startup.

This higher speed data is difficult to fully comprehend in the Bode plot. It becomes more definitive when this same data is plotted in a polar format (Figure 3).

Both Y axis probes show the primary rotor resonance at 7,800 rpm. The point of major interest is that, at full speed, the turbine-end shaft is moving towards the 9 o'clock direction, and the expander-end shaft is heading towards 4 o'clock. This behavior indicates the presence of a pivotal mode occurring at a frequency above 16,000 rpm.

In many cases, this type of response would not be unusual. However, for this unit, the historical files had no indication of a resonance around the normal running speed. Due to the response of midspan balance weights (Planes #2 and #3) at 18,500 rpm, it was clear that the vibration data was correct, and the historical undamped mode shapes were flawed.

Analytical model

As was previously stated, there are only two lateral measurement planes along the entire 2 metre (79 inch) length of this rotor. Since there were no other feasible locations for shaft probes, additional measurement options were eliminated. Therefore, the only viable approach resided with a meaningful analytical model of this rotor system.

A 65-station damped model was constructed. This computer model included bearing stiffness and damping that varied with speed, plus flexible bearing supports. The calculations produced eigenvalues (natural frequencies) plus eigenvectors (mode shapes).

The first four modes are stiff shaft pivotal and translational shapes. These modes did not appear in the vibration data due to the high dynamic stiffness for each mode. A backward mode was detected at 7,080 rpm. This mode was not visible in the startup plots, but it briefly appears as a reverse precession orbit in some of the hot coastdown data. The most active forward mode within the operating speed range occurs at a damped frequency of 7,838 rpm.

The calculated mode shapes for this resonance are shown in Figure 4. Note that the normalized deflection at both bearings are quite small. This indicates minimal motion of the journals within their respective bearings. With small relative motion, the velocity is low, and the effect of bearing damping is minimal.

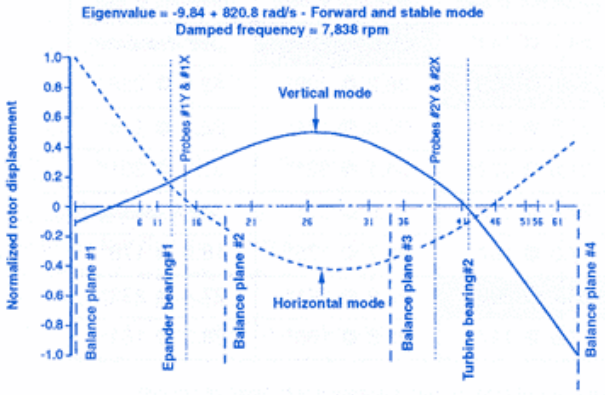

Figure 4
Calculated damped mode shapes at main rotor resonance at nominally 7,800 rpm.

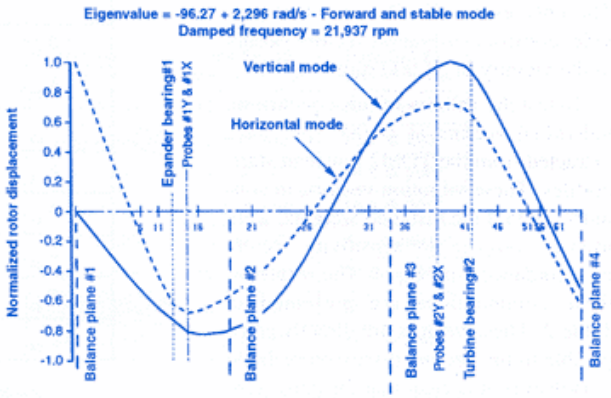

Figure 5
Calculated damped mode shapes at rotor resonance occurring above operating speed.

The validity of this analytical model is supported by the correlation of the computed resonance frequency of 7,838 rpm (Figure 4), with the measured resonance of 7,800 rpm seen in the Bode plot (Figure 2). It is also clear from Figure 4, that the rotor balance response at this resonance can be effectively controlled by corrections at the modally effective end Planes #1 and #4.

The analytical model revealed a backward mode at approximately 17,700 rpm. This pivotal mode is visible by a phase reversal (in phase to out of phase) on the transient data (Figures 2 and 3). Immediately above the normal operating speed of 18,500 rpm, a damped mode was calculated at a frequency of 21,937 rpm (Figure 5). This mode has the same deflection characteristics as the mode at 17,700 rpm. In both cases, the inboard balance Planes #2 and #3 are the most modally effective correction planes for this speed domain.

It was also concluded that weight corrections adjacent to these compressor wheels (Planes #2 and #3) should be out of phase. This was because a nodal point exists at the middle of the rotor (Figure 5) between the planes. The validity of this conclusion was field tested on the machine. The installation of a pair of weights at the middle planes at the same angle resulted in excessive vibration. However, a couple shot (out of phase) proved to be smooth, and supportive of the analytical mode shape at high speed.

Finally, the existence of a resonance at slightly above running speed, was previously noted on the polar plot (Figure 3). The analytical results shown in Figure 5 support this earlier observation. Once again, vibration measurements and the analytical tools are combined to explain the behavior of a complex machine.

Overall balance improvement

Armed with an improved understanding of the shaft response and mode shapes, plus a better appreciation of the process influence, the rotor was balanced at the intermediate speed of 14,000 rpm by using TDM2 transient data acquired during cold startups. This intermediate step was a two plane balance with weight corrections at the outboard Planes #1 and #4. This allowed the rotor to run at full speed of 18,500 rpm. A final two plane trim balance was performed on the interior Planes #2 and #3 after a full heat soak.

Transducer	Before balancing @ 14,025 rpm	After balancing @ 18,500 rpm
Expander bearing #1Y	1.41 mil pp @ 139°	0.31 mil pp @ 173°
Expander bearing #1X	1.10 mil pp @ 34°	0.50 mil pp @ 29°
Turbine bearing #2Y	0.80 mil pp @ 298°	0.11 mil pp @ 25°
Turbine bearing #2X	0.79 mil pp @ 199°	0.37 mil pp @ 192°

Table 3
Comparison of initial low speed versus final high speed runout-compensated vibration vectors.

The initial shaft vibration vectors at 14,025 rpm, and the final vectors at 18,500 rpm are shown in Table 3. The magnitude of the final running speed vectors ranged from 5 to 8% of the diametrical bearing clearance. The suitability of this balance state is demonstrated by an extended process run on this machine.

Conclusions

From the previous discussion, and the machinery example, it is clear there are some definitive guidelines that should always be considered on complex rotors. Specifically, the following items are summarized for future reference:

- Slow roll vectors, acquired under the same conditions, must always repeat. If the slow roll vectors change from run to run, then other influences or problems (e.g. a cracked shaft) should be considered.
- Transient startup and coastdown data must always be obtained. Bode and polar plots should be used to examine the 1X synchronous response for resonance and mode shape information. Spectrum cascade plots should be reviewed to verify that other frequencies are nonexistent, or are not generated as a result of the balance work.
- Balance speeds should be selected in relative plateau regions that are removed from regions that exhibit amplitude and phase variations.
- Calculations should be made for both Y axis and X axis shaft probes. When flexible supports are encountered, calculations should also be performed for the casing vibration transducers.
- Weight correction locations should be modally effective. If a weight change produces an unexpected result, the presumed mode shape may be incorrect.
- When adding (or removing) calibration weights, check the response vector ***C***. Small vector changes indicate a lack of sensitivity to the weight.
- Sensitivity vectors, acquired under similar conditions, should be consistent. If significant changes are noted, look for problems in the system.
- Care should be taken when analytically modeling the rotor system. Small mistakes or improper assumptions can result in major errors in mode shapes, and frequencies.
- Some machines, as demonstrated in this example, will require an intermediate speed, and a final trim balance speed.
- Do careful work, and be rewarded by the satisfaction of excellent results, plus the ability to "*balance a squirrel.*" ■

(Additional text in sidebar on page 19).